A Exam Question 3: Measuring Superfluid Density in Ultracold Atoms

Thomas Kiely

(Dated: February 2021)

I. INTRODUCTION

Superfluidity in condensed matter systems, such as liquid Helium, is most distinctly and straightforwardly identified by the superfluid density. While ultracold atomic systems have long realized superfluidity, however, measurement of the superfluid density has proven less natural and more elusive. It is instead straightforward to measure the condensate density of ultracold gases via time-of-flight, while superfluidity has been identified through dissipationless flow [1, 2] and vortices [3, 4]. The superfluid and condensate densities, while often considered in concert, can be quite different in many regimes of interest. The superfluid fraction, for instance, must be equal to either 1 or 0 in a Galilean-invariant system at zero temperature [5]. By contrast, the condensate density is depleted in interacting systems. Lattice systems, by breaking Galilean invariance, can realize superfluid depletion at zero temperature as well as anomalously strong superfluid drag [6]. Measuring both the condensate and superfluid densities at low temperature is an important step in characterizing the properties of ultracold gases.

Here we review proposals for measuring the superfluid fraction in ultracold atomic gases. We'll start with a (potentially long-winded) definition of superfluidity, followed by a discussion of complications that arise in cold atom systems. We will then review a few proposals and experiments that attempt to overcome these difficulties.

II. DEFINING SUPERFLUIDITY

Superfluidity is a phenomenological and collective property of matter. As such, it can be at once easy to identify and hard to define. We will first consider two thought experiments proposed by Tony Leggett [7] which will form the basis for a more rigorous and general definition.

The general setup is to consider a fluid trapped in a thin ring-shaped container. Below a critical temperature, T_c, it is understood that some (temperature-dependent) fraction of the fluid will become superfluid. This fraction vanishes as $T \to T_c$ and approaches 1 as $T \to 0$. We will imagine that we can rotate the ring at will and measure its moment of inertia. We also have control over the temperature. In the first experiment, we rotate the ring slowly (allowing the fluid to equilibrate to the motion of walls) and then we cool the temperature

below T_c. What fast and slow means will be addressed later. We then measure the moment of inertia. We will find that the measured moment of inertia, $I(T)$, divided by the rigid body value, I_0, can be continuously tuned between 0 ($T = 0$) and 1 ($T \geq T_c$) by changing the temperature. This is an equilibrium phenomenon known as the Hess-Fairbank effect [8]. The experiment has the implication that the superfluid component does not rotate with the rest of the fluid. Indeed, this is an illustration that superfluids are irrotational, which is to say that the superfluid velocity field $\vec{v}_s$ obeys $\nabla \times \vec{v}_s = 0$. Feynman and Onsager [9, 10] posited that the superfluid order parameter takes the form of a macroscopic wavefunction, $\chi(r)e^{i\phi(r)}$ and therefore the superfluid velocity is equal to $\vec{v}_s = \frac{\hbar}{m}\nabla\phi$. As the phase of the wavefunction must return to its original value modulo 2π, an application of Stokes' theorem leads to the Feynman-Onsager quantization condition

$$\oint \vec{v}_s \cdot d\vec{l} = \frac{nh}{m} \tag{1}$$

where m is the particle mass, h is Planck's constant and $n \in \mathbb{Z}$. A finite value of n implies the existence of a vortex in the velocity field. Solutions for the velocity in this case imply that $v_s(r) \sim 1/r$ where r is the perpendicular distance to the vortex. Thus, in order for the physical system to be well-defined, there must be no superfluid density at the vortex core where $r = 0$ (hence the annular trap geometry in the thought experiment). This condition implies that, at a fixed radius, the velocity of the superfluid is constrained to take certain quantized values. The Hess-Fairbank thought experiment assumes that the angular velocity of the fluid in the trap is much less than ω_0 (the $n = 1$ rotation velocity) so that the superfluid is content not to rotate with the normal fluid. It's also worth making a subtle point: the importance of the ring trap is now evident as the superfluid velocity $v_s \sim 1/r$ while the normal fluid (and the cylinder) rotate with a linear velocity $v = \omega r$. We can therefore only speak of a quantized value of the superfluid angular velocity in a trap that adequately thin so that we may ignore the irrotational nature of the superfluid. This is a simplifying feature that will show up in some of the proposals below.

The second thought experiment illustrates metastable superflow, which is a non-equilibrium phenomenon. We imagine setting the ring into motion at an angular velocity well above ω_0, allowing the fluid to equilibrate, and then cooling below T_c. We then stop the cylinder and wait. We'll find that the normal fluid, due to viscous drag from the walls, slows down and eventually comes into equilibrium with the walls of the container. The superfluid

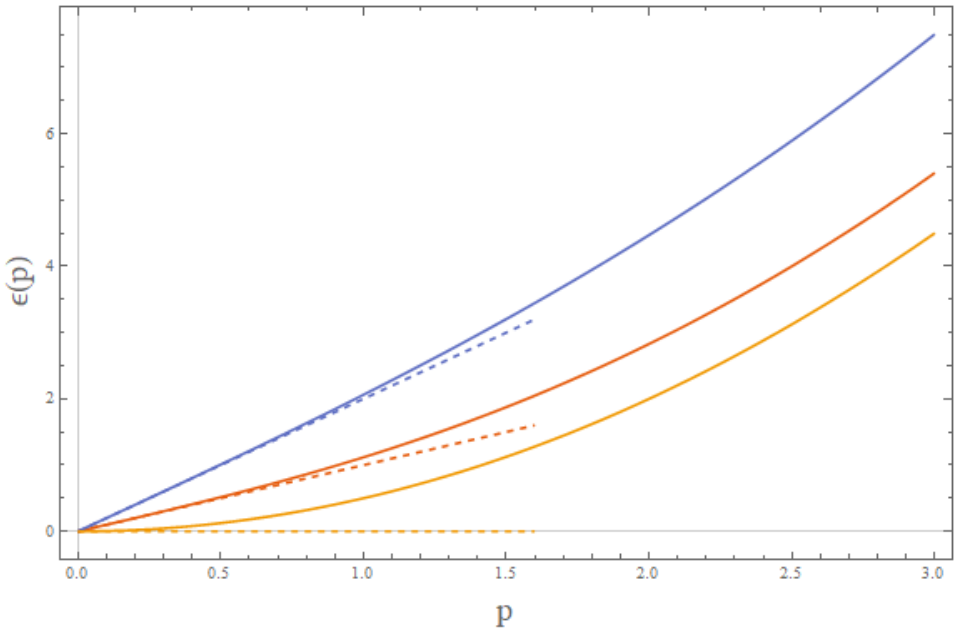

FIG. 1. Dispersion of Bogoliubov excitations in the weakly-interacting Bose gas for two finite interaction strengths (blue and red) and for the free Bose gas (orange). Dotted lines indicate the critical velocity from Eq. (2).

component, however, will continue rotating almost indefinitely. This is clearly a metastable state, as intuition would tell us that the superfluid would energetically prefer to be at rest. Quantization of superfluid rotation is clearly relevant for this experiment as well, but it would be disingenuous to provide an explanation solely on that basis. What this thought experiment illustrates is that there is some degree to which the superfluid does not feel viscous drag from the walls. Landau came up with an explanation for this phenomenon and coined the idea of a critical velocity. He imagined a Galilean-invariant system where elementary excitations have a dispersion $\epsilon(p)$. The fluid is in motion with respect to the rough walls of the container with relative velocity $\vec{v}$. The walls can generate excitations of momentum $\vec{p}$ in their own rest frame, which in the rest frame of the fluid have an energy of $\epsilon(p) + \vec{p} \cdot \vec{v}$. Therefore above a certain velocity v_c defined as

$$v_c = \min\left(\frac{\epsilon(p)}{p}\right) \tag{2}$$

the walls will generate excitations in the superfluid; for velocities below v_c the superfluid will effectively not experience drag. This condition is illustrated graphically in Fig. 1, where I have plotted a few different dispersions corresponding to the weakly-interacting Bose gas

(solid lines). The dispersion crosses over to a simple quadratic form for large momenta, so the minimum value of $\epsilon(p)/p$ is found as $p \to 0$. The dashed lines are $v_c p$ for each plot. It is shown that for the non-interacting Bose gas (orange), the critical velocity is zero. This means it does not exhibit metastability: the energy cost of creating excitations is zero. An important feature of superfluids, then, is that they are *stabilized* by interactions. Consequently, it is often said that the non-interacting Bose gas is not a superfluid (even though the superfluid fraction approaches 1 in the limit of vanishing interactions).

There are a few takeaways from this discussion. From the first thought experiment, we can see that superfluidity is formally defined in terms of the irrotational condition. This is the analog to the Meissner effect in superconductors. Phenomenologically we might identify superfluidity by the presence of vortices and by dissipationless flow, which has been done in cold atom systems. Finally, we would *characterize* a superfluid phase by its superfluid density (also known as superfluid stiffness) and by some measure of its propensity to support metastable superflow. In general Landau's original proposal for a critical velocity does not translate directly to most experimental systems, and one should instead define this stability in terms of the energy it takes to nucleate a vortex. This will depend on the geometry of the trap and on the healing length, ξ, which is the characteristic size of a vortex. Nonetheless, it is important to note that this stability condition is experimentally-relevant and distinct from the superfluid stiffness.

A formal definition of the superfluid density involves the current response to a vector potential [11]. In particular, a vector potential will couple to charged particles with an interaction Hamiltonian of the form

$$\mathcal{H}_{\text{int}} = \int d^3r \; \vec{j}(r) \cdot \vec{A}(r) \tag{3}$$

where $\vec{j}(r)$ is the particle current. In cold atom systems we will usually be thinking of neutral particles, in which case an artificial vector potential will be established via rotation or Raman dressing. By the standard linear response relations we can relate the expectation value of the current to the vector potential by defining a susceptibility. This is particularly simple upon Fourier transforming,

$$\langle j_i \rangle(k, \omega) = \chi_{ij}(k, \omega) A_j(k, \omega) \tag{4}$$

where the indices i and j denote spatial directions. The susceptibility can now be decom-

posed into transverse and longitudinal components,

$$\chi_{ij}(k,\omega) = \frac{k_i k_j}{k^2}\chi_L(k,\omega) + \left(\delta_{ij} - \frac{k_i k_j}{k^2}\right)\chi_T(k,\omega). \tag{5}$$

The superfluid density, n_s, is defined in terms of its *lack* of transverse response [11]. We have

$$\lim_{k\to 0}\chi_L(k,\omega=0) \to \frac{n}{m} \qquad \lim_{k\to 0}\chi_T(k,\omega=0) \to \frac{n_n}{m}, \tag{6}$$

where n_n is the normal fluid density and n is the total fluid density. The superfluid density, $n_s = n - n_n$, is defined as the difference between these two results.

III. COLD ATOM PROPOSALS

The classic methods of measuring the superfluid density, epitomized by Andronikashvili's torsional oscillator experiments [12, 13], consider superfluidity and superfluid density very similarly to Leggett's thought experiments. In particular, measuring the superfluid density requires that one (1) apply some rotation to the fluid at a fixed temperature and (2) measure the current response of the fluid. The current response is usually captured by the equilibrium moment of inertia: a rotating fluid contributes to the moment of inertia while non-rotating fluid does not. An appropriate definition of the superfluid density would be

$$\frac{n_s}{n} = 1 - \lim_{\omega\to 0}\left(\frac{I(\omega,T)}{I_0}\right) \tag{7}$$

where I_0 is expected moment of inertia of the device being rotated and $I(\omega,T)$ is the measured moment of inertia.

Both of the identified steps pose problems in cold atom experiments. Cold atoms are held in fixed traps generated by lasers. The force that confines them arises from the interaction between the electric field of the laser and the dipole moment of the atoms. It is clear that rotation of the lasers themselves is not an option, so alternative methods must be developed. The classic method is to induce rotation through "stirring" with a potential deformation [3, 4, 14, 15], but we will also look at proposals that induce rotation by inducing an artificial vector potential [16]. Furthermore, one cannot rely on the roughness of the walls of a container to generate viscous drag. Instead, the optical trap must lack perfect cylindrical symmetry about the axis of rotation in order to generate transverse current response. In general this will not be a major sicking point, however, as trap deformities are quite common

and can be reliably induced when necessary. The second problem involves measurement. The moment of inertia and angular momentum of a rotating disk are a straightforward quantities to measure as one can attach probes directly to the fluid-filled container. Measurements of the effective moment of inertia of a cold atom system must, again, be considerably more indirect. More fundamentally, the moment of inertia of a few thousand atoms rotating in a miniscule trap is extremely small. Even without any additional technical challenges, an analogous torsional oscillator experiment would have to be extraordinarily sensitive [17]. In general this will motivate non-mechanical (e.g. spectroscopic) methods of measuring the superfluid density.

Proposals and experiments for measuring superfluid density in cold atoms will either have to get around these particular problems or will devise altogether distinct methods. Most proposals will involve a mix of these avenues. Rather than grouping them, I will go through them sequentially in rough order of how similar they are to these classic experiments and ideas.

A. Cooper-Hadzibabic

Nigel Cooper and Zoran Hadzibabic have a proposal that most directly takes the classic rotating disk picture and translates it into the language of cold atoms [17, 18]. It is clearest to visualize this proposal in a ring-shaped trap of radius R and with a width $\Delta R \ll R$. Instead of rotating the trap, they propose using an artificial vector potential generated through Raman dressing of the hyperfine atomic states [16, 19]. We'll consider the three $F = 1$ hyperfine levels of ^{87}Rb, labeled by the quantum number $m_F = -1$, 0, and 1. Introducing a magnetic field produces a Zeeman splitting $\Delta E_m = g_F \mu_B B m_F$. The atoms are then addressed by two copropagating Laguerre-Gauss beams that couple the hyperfine levels. These beams are strongly detuned from the one-photon absorption processes. Instead, the lasers induce transitions to an excited (virtual) state, as shown in Fig. 2. The difference in frequencies between the two beams is slightly detuned from the Zeeman splitting, $\omega_1 - \omega_2 = g_F \mu_B B + \delta$, driving two-photon transitions between the hyperfine states. The Laguerre-Gauss beams carry finite orbital angular momentum [20], which we'll call l_1 and l_2. Two-photon processes such as the one shown in Fig. 2 change the orbital angular momentum of an atom by $\Delta l = l_1 - l_2$. By symmetrically driving the two hyperfine ground states as shown,

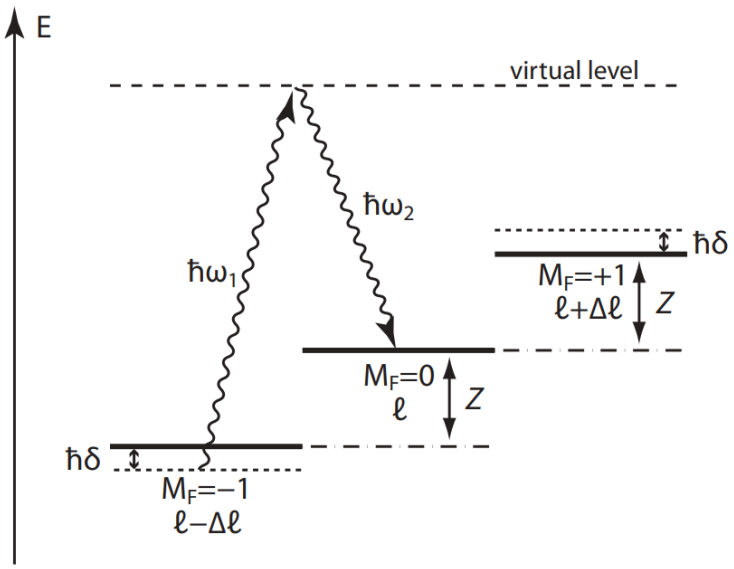

FIG. 2. Schematic for the Raman dressing of hyperfine energy levels, taken from Ref. [18]. Two beams address the atoms, driving absorption processes up to a virtual state and spontaneous emission back down to the hyperfine levels. This process adds angular momentum Δl upon transitioning between hyperfine levels.

transitions to the excited state destructively interfere with one another. This is known as electromagnetically-induced transparency (see Appendix A). We invoke the adiabatic approximation [16, 21, 22], which assumes that the system is within this "transparency window" and therefore that single-photon transitions to the excited state can be ignored. The effective Hamiltonian then couples the states $\{|m = -1, l - \Delta l\rangle, |m = 0, l\rangle, |m = 1, l + \Delta l\rangle\}$ and can be written in the rotating wave approximation [16] as

$$\begin{pmatrix} \frac{\hbar^2}{2MR^2}(l+\Delta l)^2 - \delta & \Omega_R/2 & 0 \\ \Omega_R/2 & \frac{\hbar^2}{2MR^2}l^2 & \Omega_R/2 \\ 0 & \Omega_R/2 & \frac{\hbar^2}{2MR^2}(l-\Delta l)^2 + \delta \end{pmatrix}. \tag{8}$$

The diagonal terms contain the azimuthal kinetic energy of the cold atoms in the trap in terms of the quantized angular momentum, l. The Rabi frequency Ω_R characterizes the strength of the effective coupling between hyperfine states (essentially just $\mu \cdot \mathbf{E}$). Diagonalizing the Hamiltonian yields three bands of Raman-dressed hyperfine states, each of which is minimized at a distinct value of $l/\Delta l$ as shown in Figure 3. Key to this procedure is that the separation of the bands ($\sim \Omega_R$) is presumed to be large compared to other energy scales

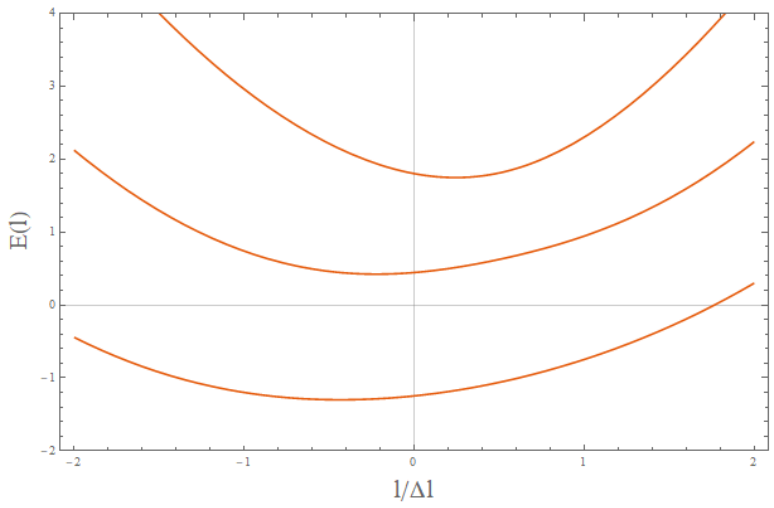

FIG. 3. Bands obtained by diagonalizing the Hamiltonian in Eq. (8) as a function of $l/\Delta l$. I've taken $\Omega_R = 2(\Delta l)^2/MR^2$ and $\delta = (\Delta l)^2/2MR^2$, and the energy is in units of $\hbar^2(\Delta l)^2/MR^2$.

in the problem. This allows the authors to assume that all atoms are in the lowest dressed band.

What we essentially have now is a method of rotating the atoms in the trap. The authors show that the part of the energy that depends on l (in the limit of large Ω_R) takes the form $\frac{\hbar^2}{M^*R^2}(l^2/2 - ll^*)$ where l^* is the value of l that minimizes the energy of the lowest band. This takes precisely the form of a Hamiltonian in a rotating frame, $\mathcal{H}_{rot} = \mathcal{H} - \vec{\omega} \cdot \vec{L}$, where in this case the effective frequency of rotation is $\omega_{\text{eff}} = \hbar^2 l^*/M^*R^2$.

The artificial vector potential now makes the laboratory frame appear as if it were a rotating frame. If we imagine gradually shifting l^* (which is proportional to $\Delta l(\delta/\Omega_R)$ at large Rabi frequencies) from 0 to some fixed value, a normal fluid would respond by rotating and then relaxing due to trap anisotropies. If ω_{eff} is kept below ω_0, the lowest quantized frequency of rotation of the superfluid, then we would find that the superfluid component of the gas *rotates* without relaxation. This is an amusing inversion of the thought experiment, but it is clear that the same principles apply.

Now we concern ourselves with measuring the superfluid density. Rather than measuring the rotational inertia, Cooper and Hadzibabic propose a spectroscopic method of extracting $\langle l \rangle$, the expectation value of the angular momentum quantum number. If all the atoms are in the normal state, we would find $\langle l \rangle = l^*$ (recall that having $l = l^*$ actually means that the particle is not moving in the laboratory frame). Defining the moment of inertia as

$\langle L \rangle = \omega_{\text{eff}} I_{\text{eff}}$, one can rewrite Eq. (7) to obtain the superfluid density as a function of $\langle l \rangle$:

$$\frac{n_s}{n} = 1 - \lim_{l^* \to 0} \left(\frac{\langle l \rangle}{l^*} \right). \tag{9}$$

Now we need a method to measure $\langle l \rangle$. Note that the lowest Raman dressed band is a superposition of the $m = -1$, 0, and 1 states. We can define the weights of each of these states as ψ_m, so $|\psi\rangle = \sum_m \psi_m |m\rangle$. The authors find through a perturbative expansion that $|\psi_{-1}|^2 - |\psi_1|^2 = p_0 + p_1 l + \mathcal{O}(l)^2$ for small angular momenta, where p_0 and p_1 are constants. Knowledge of a statistical average of these weights for the entire system would therefore be sufficient to extract $\langle l \rangle$. Fortunately, the modulus squared of these weights are just related to the probability that a particle is in a given m_F hyperfine level: e.g. $N_1/N = |\psi_1|^2$. We can measure the statistical populations of the hyperfine levels through absorption imaging, which is therefore a means of extracting the expectation value of the angular momentum. Defining the population imbalance $p = (N_{-1} - N_1)/N$, the superfluid density in the ring trap is given by

$$\frac{n_s}{n} = 1 - \lim_{l^* \to 0} \left(\frac{p - p_0}{l^* p_1} \right). \tag{10}$$

This proposal is quite clever and aesthetically pleasing in its similarities to the classic thought experiments. While it evades some of the more obvious problems we discussed at the outset, it introduces some new subtleties as well. The first is the assumption that the gas remains in the lowest Raman-dressed band. This presumes that other energy scales (chemical potential, temperature, interaction strength) are small compared to the Rabi frequency, which is related to the intensity of the Laguerre-Gauss lasers. A recent experiment realizing this rotation procedure [23] found significant population of the higher angular momentum states as a function of holding time (which is associated with residual heating). In general this can be controlled by increasing the laser intensity, but that brings about new issues: as Ω_R is increased, the absolute magnitude of $p - p_0$ decreases, thereby introducing larger experimental error. This tradeoff assessed in a subsequent paper [18] wherein the authors found a range of reasonable parameters for the weakly-interacting low-temperature Bose gas. With that said, further modeling would be necessary to determine how one might engineer a similar technique in strongly-interacting systems. The authors also claim that one could implement this scheme for a variety of trap geometries, but complications abound when one imagines scenarios in which the superfluid density is not constant in the radial direction (relative to an axis of rotation). Position-resolved absorption imaging

could potentially provide a local measure of the superfluid density, but these extensions are not addressed in detail and seem to require further assumptions. This method of inducing rotation in a trapped gas of cold atoms has been used to observe both the Hess-Fairbank effect [23] and metastable superflow [24]. The former paper used spectroscopic imaging to show the existence of a coreless vortex, but to my knowledge no group has implemented the spectroscopic measurement of the superfluid density.

B. Grimm

A similar proposal and experiment was carried out by Rudolf Grimm's group [25] on a unitary Fermi gas (UFG). The UFG is a strongly-interacting Fermi system with a diverging s-wave scattering length that exhibits paired superfluidity at low temperatures. They confine the UFG with roughly equal harmonic trapping potentials in the x and y directions and a significantly weaker harmonic trap in the z direction, resulting in a long, cigar-shaped cloud. In equilibrium, the superfluid component will sit at the center of the trap. The authors induce rotation about the z axis by applying an elliptical deformation to the trap in the x-y plane and rotating it at a fixed frequency. The normal fluid on the edges feels some friction due to the deformation and rotates in response. As long as the precessing deformation does not nucleate a vortex, the supefluid component will not rotate. In order to characterize the superfluid transition, the authors excite a radial quadrupole excitation by applying a short, *static* elliptical deformation to the trapping potential in the x-y plane. This deformation is independent of the one used to spin up the gas. They then measure the precession frequency of the mode, which is shown in Fig. 4. One might think that the mode would rotate at the frequency of the elliptic deformation, $\Omega_{\rm trap}$. This is incorrect – the static elliptic deformation excites a quadrupolar mode in the static laboratory frame, which would not precess if the gas did not have any angular momentum. The precession of this mode for a system with fast (hydrodynamic) collisions is computed in Ref. [27] and is given by $\Omega_{\rm prec} = \langle L_z \rangle / 2I_0$. Note that I_0 is the *total* rigid-body moment of inertia, including the superfluid component. This frequency can then be used to extract the angular momentum of the UFG. By dividing the precession frequency by the trap frequency, the authors define

$$\mathcal{P} = 2\,\frac{\Omega_{\rm prec}}{\Omega_{\rm trap}} = \frac{I}{I_0} \times \frac{\Omega}{\Omega_{\rm trap}} \tag{11}$$

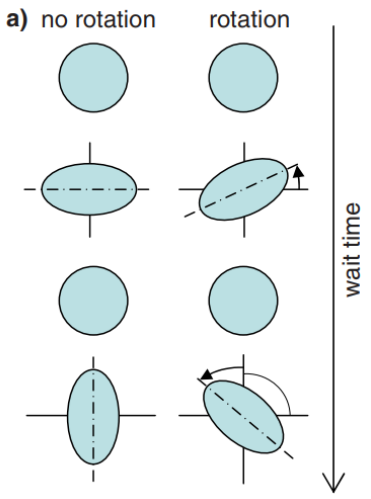

FIG. 4. Schematic of the radial quadrupole mode, taken from Ref. [26].

where Ω is rate at which the normal component of the fluid was rotating and I is the actual moment of inertia of the system (we took $\langle L_z \rangle = I\Omega$). Ideally one would have $\Omega = \Omega_{\rm trap}$, but in order to account for damping over time they leave this factor in the definition of $\mathcal{P}$. They do not explicitly state it, but it is clear that one could define a superfluid fraction $n_s/n = 1 - \mathcal{P}$ if it were reliably the case that $\Omega = \Omega_{\rm trap}$.

There are a few complications in this procedure. The first involves the definition of $\mathcal{P}$: this method requires one to identify and remove the effects of $\Omega < \Omega_{\rm trap}$ in order to get at the superfluid density. This is all the more pronounced because they introduce a time delay between the application of the static deformation and measurement of the precession frequency so that collective modes associated with the rotating elliptic deformation have a chance to damp out. This requires them to measure an average damping rate of the precession frequency (due to friction with the walls of the trap) and extrapolate backwards to determine the initial value of $\Omega_{\rm prec}$. In order to characterize and remove this Ω-dependence, they plot $\mathcal{P}$ versus the time spent in the elliptical rotation and extrapolate. The data for this procedure is shown in Fig. 5. The parameter $\mathcal{P}$ appears to saturate to a long-time value, at which point it is likely that $\Omega \approx \Omega_{\rm trap}$. Note that the authors account for the fact that long $t_{\rm spin}$ will introduce more heat into the system. In this way, the value of I/I_0 can effectively be extracted (albeit by taking a significant amount of data at a given temperature). Long spin times will in general introduce more heat into the system, but this effect seems to be manageable. Potentially more serious is the presence of vortices. The

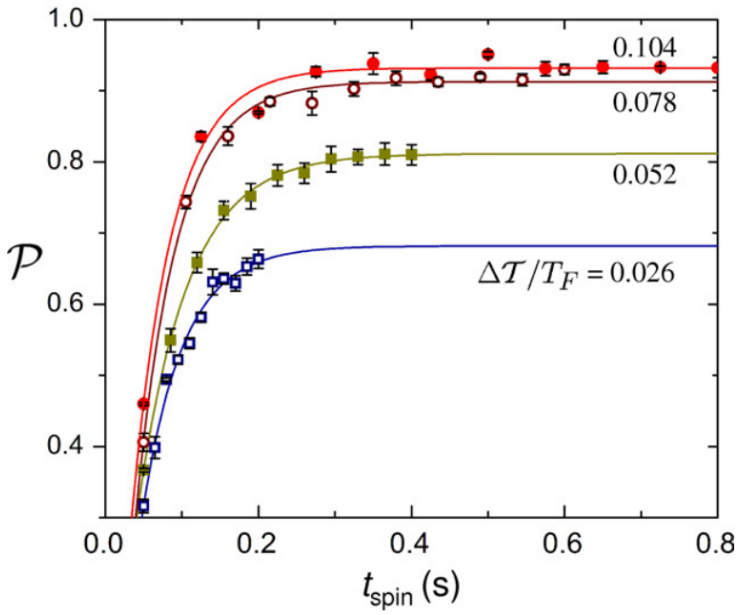

FIG. 5. Dependence on $\mathcal{P} = (I/I_0)(\Omega/\Omega_{\rm trap})$ on the time spent in the rotating elliptical deformation. Taken from Ref. [25].

authors note that resonant quadrupolar deformations are particularly effective at nucleating vortices [28], which as been taken advantage of in other contexts [3]. The deformation they introduce is weak in order to compensate for that, but in general they have no way of determining if a vortex has formed in the superfluid core. Finally, this procedure only works for systems where the superfluid and normal components can be described hydrodynamically. The strong interactions of the UFG mean that this is a reasonable assumption, but it would be incorrect to apply this method to the weakly-interacting Bose gas. This is not necessarily a positive or a negative feature, but it's worth keeping in mind that this procedure is not universally-applicable.

C. Ho-Zhou

A paper by Tin-Lun Ho and Qi Zhou [29] presents a local detection scheme based on the column-integrated density of a harmonically-trapped gas. The column-integrated density (e.g. $n(x,y) = \int n(x,y,z)\ dz$) is one of the few local observables that can be extracted in cold atom experiments. The geometry they envision is a harmonically-confined 3D trapped gas where $\omega_x \approx \omega_y \neq \omega_z$, but these conditions are not strictly necessary.

The authors make extensive use of the local density approximation, which assumes that the local properties of a gas in an inhomogeneous trap are related to the bulk thermodynamic equation of state. Considering a trapped gas with chemical potential $\mu(\mathbf{r}) = \mu - V(\mathbf{r})$, the local density approximation amounts to the statement that

$$n(\mathbf{r}) = n(\mu(\mathbf{r}), T) \tag{12}$$

where $n(\mu, T)$ is the density of the bulk homogeneous system. This approximation has been shown to be quite accurate in ultracold atomic systems [30] and is widely used. The first thing we will show is how to get from the column-integrated density, $\bar{n}(x, y)$ back to the 3D density, $n(x, y, z)$ (the authors cite Erich's contribution in this derivation). Starting with the Gibbs-Duhem relationship, $dP = n\ d\mu + s\ dT$, we have that $P = \int n\ d\mu$ at fixed temperatures. By rewriting the average density as a function of x,

$$\begin{aligned}
\bar{n}(x) = \int dydz\ n(x,y,z) &= \int dydz\ n\big(\mu - (M/2)\sum_i \omega_i^2 x_i^2, T\big) \\
&= \frac{2}{M\omega_y\omega_z}\int d\tilde{y}d\tilde{z}\ n\big(\mu - (M/2)\omega_x^2 x^2 - \tilde{y}^2 - \tilde{z}^2, T\big) \\
&= \frac{1}{M\omega_y\omega_z}\int d(\tilde{r}^2)d\tilde{\theta}\ n\big(\mu - (M/2)\omega_x^2 x^2 - \tilde{r}^2, T\big) \\
&= \frac{2\pi}{M\omega_y\omega_z}\int_x d\mu\ n(\mu, T),
\end{aligned} \tag{13}$$

we can obtain the following relationship for the pressure:

$$P(x,0,0) = \frac{M\omega_y\omega_z}{2\pi}\bar{n}(x). \tag{14}$$

Note that $\int_x$ means that the boundary conditions of the integral are offset by $(M/2)\omega_x^2 x^2$. We can then use the Gibbs-Duhem relation again to find

$$n(x,0,0) = \left(\frac{\partial P}{\partial \mu}\right)_T = \frac{\partial P(x,0,0)}{\partial x}\left(\frac{\partial \mu(\mathbf{r})}{\partial x}\right)^{-1} = -\frac{1}{2\pi x}\frac{\omega_y\omega_z}{\omega_x^2}\ \frac{\partial \bar{n}(x)}{\partial x}. \tag{15}$$

Manipulations like these, taking us from integrated quantities to bulk thermodynamic quantities using the local density approximation, are the basis of this proposal.

Now, to address the case of a finite superfluid density, the authors consider a system that is in motion. The velocity of the normal component is $\mathbf{v}_n$ and that of the superfluid component is $\mathbf{v}_s$; their difference is $\mathbf{w} = \mathbf{v}_s - \mathbf{v}_n$. In the frame moving with $\mathbf{v}_n$, the Gibbs-Duhem relationship can be rewritten as

$$dP = n\ d\mu_0 + s\ dT - Mn_s\mathbf{w}\cdot d\mathbf{w} \tag{16}$$

where n_s is the superfluid number density and μ_0 is the chemical potential in the $\mathbf{v}_n = 0$ frame. The last term can just be thought of as a kinetic energy – a momentum density of the superfluid times its velocity. They proceed to perform the same sort of manipulations in the small-w limit to obtain an equation for the superfluid density as a function of position, $n_s(x, 0, 0)$, in terms of the column-integrated densities with and without rotation. The calculation itself is notationally a bit confusing so I will refrain from going into further details. The key feature, however, are that one can compute the superfluid density as a function of position in the full 3D system using two column-integrated density profiles: one while the system is stationary and one while applying a slow rotation.

This method is intriguing because it proposes a *local* measurement of the superfluid density, unlike the previous proposals. The authors also make use of a particular local measurement, the column-integrated density, which can be reliably performed. One potential shortcoming of this procedure is its assumptions of thermal equilibrium in the presence of rotation. This is, however, also an implicit assumption in the other schemes presented until now. One should additionally be cautious about applying the local density approximation to systems in which the correlation length diverges [31–33] and for strongly-interacting systems on lattices [34]. This might exclude or complicate the application of this method to certain "interesting" systems. For a wide variety of systems, however, this method provides a means to efficiently measure the superfluid density as a function of position. While it has not (to the best of my knowledge) been used to compute the superfluid fraction, a recent experiment [35] used the column-integrated density to compute the equation of state of a weakly-interacting 3D Bose gas.

D. Carusotto-Castin

We now step away from direct analogs of the equilibrium thought experiments. A paper by Iacopo Carusotto and Yvan Castin [36] proposes the use of spatially-localized artificial gauge fields to measure the local superfluid density. This proposal, unlike the previous ones, does not assume thermal equilibrium.

The authors envision a pancake-shaped trap that is tightly-confined in the $\hat{z}$ direction. The atoms themselves have two hyperfine levels, $|a\rangle$ and $|b\rangle$, whose energies have been split using a magnetic field. They address the atoms with three lasers: a control laser $(\Omega_c, \mathbf{k}_c)$,

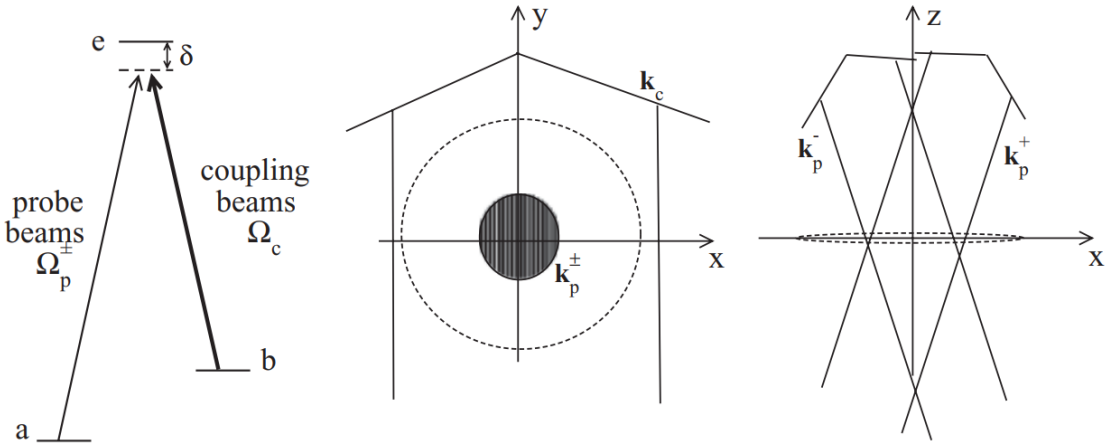

FIG. 6. Figure showing the schematic Raman driving procedure as well as the physical geometry of the trap and lasers. The black circle is the location of the atoms. Taken from Ref. [36].

which drives from $|b\rangle$ to an excited state $|e\rangle$ with some detuning δ, and two probe lasers $(\Omega_p^{\pm}, \mathbf{k}_p^{\pm})$ that drive from $|a\rangle$ to $|e\rangle$ with the same detuning (see Fig. 6). The control laser momentum is pointed along the $\hat{y}$ direction, as shown, and the probe laser momenta are given by $\mathbf{k}_p^{\pm} = k_p\hat{z} \pm \mathbf{q}/2$ where $\mathbf{q}$, their difference, lies in the x-y plane. The probe lasers are Gaussian lasers with a waist w that is considerably smaller than the radius of the trapped gas. This allows for local measurements to be made. They note, however, that the waist must also be much larger than the healing length, ξ, of the trapped gas. This makes an important point – superfluidity is a macroscopic (collective) phenomenon, so any "local" probe of the superfluid density must be larger than some microscopic length scale in order to observe bulk superfluid effects. It is not explicitly state, but a caveat to the claim that the fluid need not be in thermal equilibrium is that there must be *local* thermal equilibrium on these same length scales. This microscopic length scale is the healing length, which is the characteristic length scale of the vortices. In the weakly-interacting Bose gas, $\frac{\hbar^2}{m\xi^2} = \rho g$ where g is the interaction strength.

Returning to the Raman driving procedure, it is assumed that the control and probe beams are far detuned from any hyperfine transitions so we can consider the two-photon process as an effective coupling between $|a\rangle$ and $|b\rangle$. The authors show that this realizes an

artificial vector potential in the $\hat{y}$ direction (c.f. Sec. III A, Appendix A), given by

$$A_y(\mathbf{r}) = \hbar k_c \frac{|\Omega_p^+|^2 + |\Omega_p^-|^2 + |\Omega_p^+(\Omega_p^-)^* e^{i\mathbf{q}\cdot\mathbf{r}/2} + h.c.|}{|\Omega_c|^2} e^{-2|\mathbf{r}-\mathbf{r}_0|^2/w^2}. \tag{17}$$

To the extent that one can subtract off or ignore the $|\Omega_p^+|^2 + |\Omega_p^-|^2$ term, this vector potential can be either transverse or longitudinal depending on whether $\mathbf{q} \perp \hat{y}$ or $\mathbf{q} \parallel \hat{y}$, respectively (recall $\mathbf{k}_c = k_c\hat{y}$). The part we want to ignore is unmodulated (a constant function of $\mathbf{r}$) and always contributes to the longitudinal part of the vector potential. Notice that the vector potential has a Gaussian envelope confining it to the point $\mathbf{r}_0$ (the center of the probe beams) with a waist w, allowing us to apply a local perturbation.

From Sec. II we know that the total density will respond to the longitudinal vector potential while only the normal component will respond to a transverse vector potential. In both cases it is required that we take the long-wavelength limit, which is satisfied for $q\xi < 1$. Thus, the authors have realized a clever way of locally distinguishing the superfluid density. The question now is how to detect the response. The central issue, clear from the tenets of linear response, is that a small vector potential means a proportionately small current response. Note of course that "small" is not just referring the magnitude of A_y: by only acting on a local region of width w near $\mathbf{r}_0$, current will only be generated within that region.

The authors propose two methods for detection. In both, they continuously irradiate the atoms with the coupling laser but pulse the probe laser with time dependence $\Theta(t)e^{-\gamma t}$: the laser turns on at $t = 0$ and then exponentially decays. The reason for the decay is that, if the local vector potential is applied for too long, non-linear couplings will prevent one from distinguishing the local superfluid density. They decay rate also cannot be too short, however, because the system must have time to respond to the perturbation. The response time is set by the sound velocity of the Bose gas, and thus it should be no surprise that the constraint fixes $\gamma/c_s q$ (the authors show that a value of 10^{-1} or less gives accurate measurements). For more complicated systems where such a calculation isn't possible, the decay rate γ may have to be calibrated in the experiment.

The first method relies on the fact that the energy deposited into the trapped gas by turning on the probe laser depends on the current response. Specifically, through linear response relations and the local density approximation they find that the added energy $\Delta E \propto \rho_n(\mathbf{r}_0)$ for $\mathbf{q} \perp \hat{y}$ and $\Delta E \propto \rho(\mathbf{r}_0)$ for $\mathbf{q} \parallel \hat{y}$. The unmodulated contribution to the energy can be removed by making measurements at different angles $\mathbf{q} \cdot \hat{y}$. Measuring the

change in energy would involve imaging the density profile before and after a time-of-flight expansion, which has been used to measure the equation of state of Fermi [37] and Bose [38] gases. They find that their linear response result is valid out to energies of approximately

$$\delta E_{\max}(\rho) \approx 0.1 \times \left(\frac{\pi}{4} w^2 \rho \; k_B T_d \right) \tag{18}$$

where ρ can be either the normal fluid density or the total density based on the conditions above and $T_d = 2\pi\hbar^2\rho/m$ is the degeneracy temperature. Recall that w^2 is roughly the area of the region on which the vector potential is applied, so there is a clear tradeoff between locality and a discernible change in energy. It would likely not be possible to distinguish energies below a percent of $k_B T_d$ [35], which would constrain the total number of particles addressed by the field $w^2\rho \sim \mathcal{O}(10)$. Of course this result is density-dependent, so it's possible one could do better.

The second method for measuring the local current response is through optical imaging. The authors propose measuring the intensity of the probe laser after it passes through the sample. In making the adiabatic approximation, we assumed a phenomenon called electromagnetically-induced transparency (see Appendix A) in which destructive interference from the symmetric driving of the coupling and probe beams decouples the Raman-dressed states from the lasers altogether [16, 19, 22]. This will hold true when the atoms are at rest, and consequently the probe beam is not scattered by the sample. Atomic motion can throw a wrench in things, however, by introducing a Doppler shift [39]. The resulting asymmetry seen by the atom leads to a small coupling between the dressed state and the bare excited state. This coupling naturally means that the atoms have a finite dipole polarization that can act as a source term to the electric field of the probe laser. The authors show that the change in light intensity is proportional to the expectation value of the current $\langle \mathbf{j}(\mathbf{r}) \rangle$. Measuring the intensity of transmitted light for longitudinal and transverse vector potentials therefore provides a means to measure the superfluid density. As with the previous method, there are unwanted effects arising from an additional motional coupling to the density gradient and from the unmodulated component of the vector potential. It is argued that the former can be ignored because it is orders of magnitude smaller than the contribution of the current, while the latter would again require angle-resolved measurements to subtract off the unwanted component. The effect would require measuring fractional changes in the intensity of the transmitted light that are on the order of 10^{-7}, which would be near the standard quantum

limit for a gas of $\mathcal{O}(10^6)$ atoms.

This proposal is a clever extension of the ideas developed in previous sections to a non-equilibrium, local setting. Furthermore, the locality of the measurement method indicates that similar measurements should (ostensibly) be feasible in any quasi-2D trap geometry, including on a lattice. With that said, there are two primary caveats. The first is that applications of this technique to "interesting" systems or to lattice models would either require extensive calibration or theoretical modeling to determine the range of appropriate parameters. For example, it would take a variety of measurements to determine the dependence on $\mathbf{q} \cdot \hat{y}$ and reasonable values for γ and $\mathbf{q}$ in the absence of reliable modeling. The second caveat is that the authors do not get around the "smallness" problem stated at the outset. It appears that truly local measurements using this technique would have to be extremely precise and would therefore likely be quite noisy.

E. Second Sound

Finally, I will present the work of two groups that measured the superfluid fractions of the unitary Fermi gas [40] and the 2D Bose gas [41], respectively, by measuring the velocities of first and second sound. This is a method which is experimentally quite robust insofar as it does not depend on thermal equilibrium during rotation. Its major drawback, however, is that it requires extensive knowledge of bulk thermodynamic properties. In these cases, the experimental groups were able to determine these properties using just the temperature and interaction strength due to prior theoretical modeling. For this reason, this method is of reasonably limited applicability.

The model of a finite temperature superfluid as consisting of coexisting normal and superfluid components was proposed by Tisza [42] and Landau [43] and is aptly called the two-fluid model. This assumption naturally leads to the prediction of two low-energy sound modes: first sound, which is a propagating compression mode, and second sound, an isobaric mode where the normal and superfluid components oscillate out of phase [44]. These can be thought of as a propagating density mode and a propagating heat/entropy mode, respectively. The velocities of these quantities are determined by the solutions to the quartic equation [41, 45]

$$c^4 - (\tilde{c}_1^2 + \tilde{c}_2^2)c^2 + \tilde{c}_1^2\tilde{c}_2^2/\gamma = 0 \tag{19}$$

where

$$\tilde{c}_1^2 = \frac{1}{mn\kappa_s} \qquad \tilde{c}_2^2 = \frac{T\bar{s}^2 n_s}{mn_n c_V} \qquad \gamma = \frac{\kappa_T}{\kappa_s} \tag{20}$$

are parameters fixed by the thermodynamic properties of the system. In the above we identify $\bar{s}$ as the entropy per particle, κ_s (κ_T) as the adiabatic (thermal) compressibilities, and c_V as the specific heat per particle at constant volume. These are the parameters that have been determined for the unitary Fermi gas [44] and the 2D Bose gas [46] as functions of T/T_F and T/T_c, respectively. In the case of these experiments, the solutions to the quartic equation are used to determine the superfluid density n_s.

We will assume that these parameters or functions are known, turning to the problem of how to measure the sound veocities. In Ref. [40], the authors confine a unitary Fermi gas to a cigar-shaped trap. They excite a first-sound mode by suddenly generating a localized "bump" in the potential using a tightly-focused laser. They then take images of the density as a function of time in the elongated direction of the trap to extract the sound velocity. The second-sound mode is more tricky: they load the gas with the localized bump already present in the trapping potential and then quickly modulate the power of the laser to drive the system locally out of equilibrium. The sinusoidal modulation maintains the same average potential height so that they don't excite a first sound mode. They then halt the modulation and allow the system to relax. As the system relaxes, the local temperature and entropy perturbation propagates outward. They then measure the velocity of the temperature wave by imaging the density as a function of time, identifying a decrease in the density as a region of locally-increased temperature. This is a clever and physically-intuitive measurement, although the results are rather noisy. Their data for the superfluid density as a function of temperature are shown in Fig. 7 alongside the superfluid density of Helium II (green) and the Bose-Einstein condensate fraction (red). Horizontal uncertainty arises from the challenge of determining the temperature of trapped gases in general as well as from finite-size effects, which can shift T_c by $\sim 10\%$.

In Ref. [41], the authors study a quasi-2D Bose gas in a box trap: a hollow laser beam is used to confine the atoms to a box $L_x \times L_y$ in the x-y plane, and a tight harmonic trap confines the atoms in the z direction. As the system is cooled, it is predicted to undergo a BKT transition into the superfluid phase. This transition is associated with the condensation of vortices and can be characterized by a discontinuous jump in the superfluid density [47]. They will choose to plot the superfluid phase space density, $D_s = n_s\lambda_T^2$ where

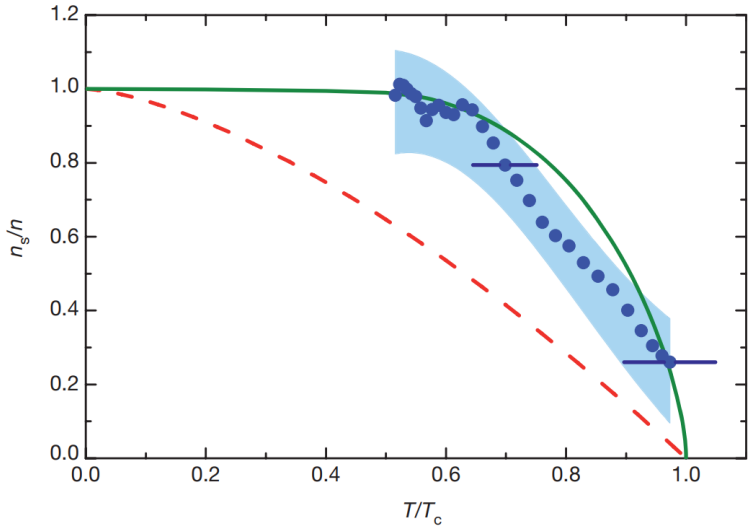

FIG. 7. Superfluid fraction versus temperature obtained by measuring the second sound in the unitary Fermi gas. Also shown are the superfluid fraction of Helium II (green) and the condensate fraction of a Bose gas (red). Taken from Ref. [40].

λ_T is the deBroglie wavelength. In these units, the magnitude of the jump is 4 (D_s is dimensionless). In order to extract the sound velocities, they measure the long-wavelength density response of the gas to a spatially-uniform, in-plane force $F_y(t) = F_0 \sin(\omega t)$ generated by a magnetic field gradient. Measuring the out-of-phase oscillations in the center of mass of the gas then characterizes the absorptive response, which can be related to the dynamical structure factor, $S(\omega, q_L)$. The wavelength of the excitations $q_L = 2\pi/L_y$ corresponds to the longest-available wavelength in the box trap. They can then identify peaks in the dynamical structure factor as sound modes. They find two peaks in the superfluid phase, $\omega_{1,2}$, resulting in first and second sound velocities $c_{1,2} = \omega_{1,2}/q_L$. Upon transitioning into the normal phase, the second sound mode (the lower of the two frequencies) becomes an overdamped diffusive mode. Inserting their measured sound velocities into the Eq. (19), they are able to extract the superfluid density. Their data is shown in Fig. 8 where they plot D_s versus $D = n\lambda_T^2$, the total phase space density. The solid curve is a theoretical prediction with no free parameters, and the dotted line corresponds to a superfluid fraction of 1. There is clearly an impressive agreement, even resolving the jump in the superfluid density across the transition.

As was made clear at the outset of this section, this is a specialized method for computing the superfluid density. It relies on extensive theoretical modelling which, in these cases, was

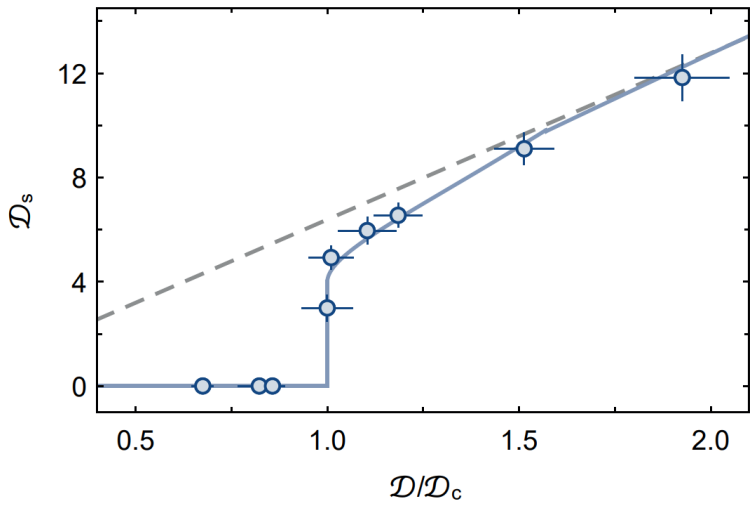

FIG. 8. Plot of the superfluid phase space density versus the total phase space density using values extracted from measurements of the sound velocities. Theory curve is the result for the infinite 2D Bose gas with no free parameters and dashed line indicates a superfluid fraction of 1. Taken from Ref. [41].

simplified by the universality of the systems at hand. While in some cases this could be substituted for an experimental determination of the equation of state, this would likely come at the cost of significantly larger error bars and would make the method much more cumbersome. With that said, introducing a density perturbation and imaging the density response over time is a comparatively "natural" procedure in cold atom experiments.

IV. FINAL REMARKS

The question of how to compute the superfluid density in ultracold atomic gases is not necessarily a new question, but it is gaining relevance as experimentalists seek to study transport properties in finely-tuned "model" systems [48, 49]. These properties, which include the conductivity, are not necessarily natural observables in the context of cold atoms. The proposals reviewed above each try to circumvent the technical difficulties involved in measuring a macroscopic, equilibrium phenomenon in a small, thermally-closed system.

The first three sections review proposals that can be understood as more complicated variants of Tony Leggett's thought experiments. The Grimm group's experiment attempts to stir the cold gas with a trap deformation, which has the drawbacks of heating the system

and likely introducing collective modes. Their method of measurement, while clever, may also introduce vortices; this would be a fatal flaw when measuring the superfluid density. The method is also limited to strongly-interacting quantum fluids in the hydrodynamic regime, which could be viewed as a weakness or a strength. The Cooper-Hadzibabic proposal imposes slow rotation using an artificial gauge field, which should in theory be less disruptive than a rotating deformation. While the measurement procedure they present is limited to the ring trap geometry, the spectroscopic method is convenient and has already been used in another context [23]. It is an open question whether this measurement method would be feasible in a strongly-interacting system, however, as the requirement that Ω_R be greater than all other energy scales would mean that the magnitude of observables should shrink proportionately. Equally convenient is the algorithm proposed by Ho and Zhou, which only requires a snapshot of the column-integrated density. This seems like the most versatile of the proposed methods of measurement, although the noise associated with inverting the column-integration is not insignificant [35]. In concert with the experimental procedure set out in Ref. [17] and realized in Ref. [23], measurement of the superfluid density as a function of position in a harmonic trap should already be feasible.

We then examined two alternative procedures. The first, a proposal by Carusotto and Castin, provides a means to measure superfluid density locally via a tightly-confined artificial vector potential. This has the benefit of not requiring thermal equilibrium, which can be a significant burden in small closed quantum systems. While the probing techniques are within reach, precise measurements of the small current response would require very high sensitivity. For that reason, this method does not yet seem realizable. In the last section, we reviewed two experiments that extracted the superfluid density from the second sound velocity. The experimental methods in both cases were natural and broadly-applicable. The methods of Ref. [41] bear a resemblance to those recently employed to measure the conductivity of a 2D Fermi-Hubbard system in an optical lattice [50], a demonstration of their versatility in cold-atom transport problems. The drawbacks of this method, requiring knowledge of the thermodynamic properties of the system, could be quite severe. With that said, the methods of Ref. [41] seem particularly valuable given the ability to broadly characterize the long-wavelength collective modes of the system. Advances in quantum gas microscopy and model-free thermometry [51] could improve experimental determinations of the equation of state to make this a viable method for measuring the superfluid density.

A. Post-Exam Comments

Worth also keeping in mind that one can engineer Peierls phases using artificial vector potentials, which could be a useful application/proposal in 1D.

Also, in the introduction, it's useful to distinguish phase stiffness from something like Cooper pair density. Debanjan pointed out a distinction in superconductors that's useful to keep in mind. The phase stiffness, which I generally denote as n/m^*, in a BCS superconductor is the delta function weight in $\sigma(\omega)$. The function $\sigma(\omega)$ for a superconductor has a gap of 2Δ (with a factor of 2 because it's a 2-particle response function) and a delta function peak at $\omega = 0$. This latter feature is what distinguishes superconductors from insulators. The weight of the delta function is the phase stiffness, which is proportional to the square of the penetration depth (in BCS theory). I admit I'm a little lost on where he was going with this. The superfluid density n_s/m^* is defined similarly, and one ought to be careful to argue that it does not correspond to the Cooper pair density. That much is clear. He then claimed that the phase stiffness, which is related to SF density, is independent of the gap Δ at zero temperature. Whether this is what he meant is unclear, as the phase stiffness could be related to the rest of the conductivity through a sum rule, which might naively suggest that there would be a gap dependence. I'm not sure if he meant Cooper pair density instead.

Appendix A: Electromagnetically-Induced Transparency

Here I'll make some very brief comments on the phenomenon of electromagnetically-induced transparency, largely taken from Ref. [22]. This is relevant for the Cooper-Hadzibabic (Sec. III A) and Carusotto-Castin (Sec. III D) proposals.

Consider a gas of atoms with two hyperfine "ground state" levels, $|g\rangle$ and $|s\rangle$, which differ in energy of order the Zeeman splitting, and an excited state level, $|e\rangle$. This is a simplified version of the schemes used in the above proposals and is shown schematically in Fig. 9. Generically if one shines coherent laser light on the cloud of atoms with a frequency $\hbar\Omega_{\text{signal}} = E_e - E_g$, the light will be absorbed as it drives transitions between $|g\rangle$ and $|e\rangle$. The medium would therefore be opaque, as this process will lead to the absorbed light being scattered as the excited state decays. If one were to also shine a laser on the system with frequency $\hbar\Omega_{\text{control}} = E_e - E_s$, one might expect things to get even more complicated. Interestingly,

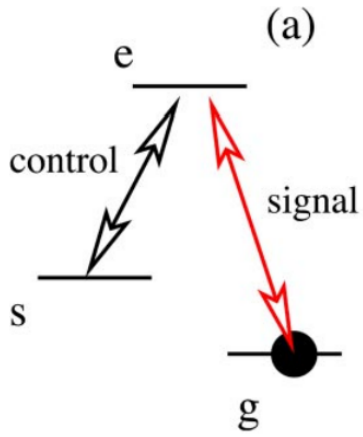

FIG. 9. Plot of the three-level system being considered here with symmetric driving of two distinct hyperfine ground states into the same excited state. Taken from Ref. [22].

however, one instead finds that such a procedure leads to destructive interference in the transitions between the respective ground states and the excited state. More concretely, one can write down the Hamiltonian for this three-level system with the two coherent drives and find that there is an eigenstate that is completely decoupled from the excited state. This eigenstate, a linear combination of the hyperfine ground states, is known as a dark state. As the excited state will decay with a shorter lifetime than the ground states, continuously driving the system will pump the system into the dark state. When the system is in the dark state, it is no longer scattering the laser light – thus, we have the phenomenon of electromagnetically-induced transparency.

We make use of similar schemes when considering the use of artificial vector potentials. The general idea is that we drive the system symmetrically, as shown here, and the low-energy features of the resulting model will not involve the excited state at all. One can then ignore the excited state and consider the truncated Hilbert space that just involves the ground state hyperfine levels. This is, of course, only valid for coherent drives that are adequately symmetric and close to the resonance. The assumption that all the relevant dynamics occur within this "transparency window" is what we refer to as the adiabatic

approximation [22].

---

[1] C. Raman, M. Köhl, R. Onofrio, D. S. Durfee, C. E. Kuklewicz, Z. Hadzibabic, and W. Ketterle, Phys. Rev. Lett. **83**, 2502 (1999).

[2] C. Ryu, M. F. Andersen, P. Cladé, V. Natarajan, K. Helmerson, and W. D. Phillips, Phys. Rev. Lett. **99**, 260401 (2007).

[3] K. W. Madison, F. Chevy, W. Wohlleben, and J. Dalibard, Phys. Rev. Lett. **84**, 806 (2000).

[4] J. R. Abo-Shaeer, C. Raman, J. M. Vogels, and W. Ketterle, Science **292**, 476 (2001), https://science.sciencemag.org/content/292/5516/476.full.pdf.

[5] A. Leggett, J. Stat. Phys. **93**, 927–941 (1998).

[6] V. M. Kaurov, A. B. Kuklov, and A. E. Meyerovich, Phys. Rev. Lett. **95**, 090403 (2005).

[7] A. J. Leggett, Rev. Mod. Phys. **71**, S318 (1999).

[8] G. B. Hess and W. M. Fairbank, Phys. Rev. Lett. **19**, 216 (1967).

[9] R. P. Feynman, Rev. Mod. Phys. **29**, 205 (1957).

[10] L. Onsager, Nuovo Cim **6**, 279–287 (1949).

[11] D. J. Scalapino, S. R. White, and S. Zhang, Phys. Rev. B **47**, 7995 (1993).

[12] E. Andronikashvili, Zh. Exp. Teor. Fiz. **18**, 424–431 (1948).

[13] E. Andronikashvili and Y. Mamaladze, Prog. Low Temp. Phys. **5**, 79 (1967).

[14] N. Cooper, Advances in Physics **57**, 539 (2008), https://doi.org/10.1080/00018730802564122.

[15] A. L. Fetter, Rev. Mod. Phys. **81**, 647 (2009).

[16] I. B. Spielman, Phys. Rev. A **79**, 063613 (2009).

[17] N. R. Cooper and Z. Hadzibabic, Phys. Rev. Lett. **104**, 030401 (2010).

[18] S. T. John, Z. Hadzibabic, and N. R. Cooper, Phys. Rev. A **83**, 023610 (2011).

[19] R. Dum and M. Olshanii, Phys. Rev. Lett. **76**, 1788 (1996).

[20] F. Pampaloni and J. Enderlein, Gaussian, hermite-gaussian, and laguerre-gaussian beams: A primer.

[21] J. Dalibard, F. Gerbier, G. Juzeliūnas, and P. Öhberg, Rev. Mod. Phys. **83**, 1523 (2011).

[22] M. D. Lukin, Rev. Mod. Phys. **75**, 457 (2003).

[23] P.-K. Chen, L.-R. Liu, M.-J. Tsai, N.-C. Chiu, Y. Kawaguchi, S.-K. Yip, M.-S. Chang, and Y.-J. Lin, Phys. Rev. Lett. **121**, 250401 (2018).

[24] C. Ryu, M. F. Andersen, P. Cladé, V. Natarajan, K. Helmerson, and W. D. Phillips, Phys. Rev. Lett. **99**, 260401 (2007).

[25] S. Riedl, E. R. S. Guajardo, C. Kohstall, J. H. Denschlag, and R. Grimm, New Journal of Physics **13**, 035003 (2011).

[26] S. Riedl, E. R. S. Guajardo, C. Kohstall, J. H. Denschlag, and R. Grimm, Phys. Rev. A **79**, 053628 (2009).

[27] F. Zambelli and S. Stringari, Phys. Rev. Lett. **81**, 1754 (1998).

[28] N. G. Parker and C. S. Adams, Phys. Rev. Lett. **95**, 145301 (2005).

[29] T. Ho and Q. Zhou, Nature Phys **6**, 131–134 (2010).

[30] N. Gemelke, X. Zhang, C. Hung, and C. Chin, Nature.

[31] S. Bergkvist, P. Henelius, and A. Rosengren, Phys. Rev. A **70**, 053601 (2004).

[32] K. W. Mahmud, E. N. Duchon, Y. Kato, N. Kawashima, R. T. Scalettar, and N. Trivedi, Phys. Rev. B **84**, 054302 (2011).

[33] L. Pollet, N. V. Prokof'ev, and B. V. Svistunov, Phys. Rev. Lett. **104**, 245705 (2010).

[34] J. Carrasquilla and M. Rigol, Phys. Rev. A **86**, 043629 (2012).

[35] C. Mordini, D. Trypogeorgos, A. Farolfi, L. Wolswijk, S. Stringari, G. Lamporesi, and G. Ferrari, Phys. Rev. Lett. **125**, 150404 (2020).

[36] I. Carusotto and Y. Castin, Phys. Rev. A **84**, 053637 (2011).

[37] N. Navon, S. Nascimbène, F. Chevy, and C. Salomon, Science **328**, 729 (2010), https://science.sciencemag.org/content/328/5979/729.full.pdf.

[38] S. P. Rath, T. Yefsah, K. J. Günter, M. Cheneau, R. Desbuquois, M. Holzmann, W. Krauth, and J. Dalibard, Phys. Rev. A **82**, 013609 (2010).

[39] A. Aspect, E. Arimondo, R. Kaiser, N. Vansteenkiste, and C. Cohen-Tannoudji, Phys. Rev. Lett. **61**, 826 (1988).

[40] L. Sidorenkov, M. Tey, R. Grimm, Y.-H. Hou, L. Pitaevskii, and S. Stringari, Nature **498**, 78–81 (2013).

[41] P. Christodoulou, M. Gałka, N. Dogra, R. Lopes, J. Schmitt, and Z. Hadzibabic, Observation of first and second sound in a berezinskii-kosterlitz-thouless superfluid (2020), arXiv:2008.06044 [cond-mat.quant-gas].

[42] L. Tisza, CR Acad. Sci **207**, 1035 (1938).

[43] L. Landau, Physical Review **60**, 356 (1941).

[44] Y.-H. Hou, L. P. Pitaevskii, and S. Stringari, Phys. Rev. A **88**, 043630 (2013).

[45] M. Ota and S. Stringari, Phys. Rev. A **97**, 033604 (2018).

[46] N. Prokof'ev and B. Svistunov, Phys. Rev. A **66**, 043608 (2002).

[47] R. Fletcher, Bose-einstein condensation and superfluidity in two dimensions (2015).

[48] C. Chien, S. Peotta, and M. Di Ventra, Nature Phys **11**, 998–1004 (2015).

[49] J. Stajic, Science **363**, 360 (2019), https://science.sciencemag.org/content/363/6425/360.2.full.pdf.

[50] P. T. Brown, D. Mitra, E. Guardado-Sanchez, R. Nourafkan, A. Reymbaut, C.-D. Hébert, S. Bergeron, A.-M. S. Tremblay, J. Kokalj, D. A. Huse, P. Schauß, and W. S. Bakr, Science **363**, 379 (2019), https://science.sciencemag.org/content/363/6425/379.full.pdf.

[51] T. Hartke, B. Oreg, N. Jia, and M. Zwierlein, Phys. Rev. Lett. **125**, 113601 (2020).